Journal of Molecular Graphics and Modelling 38 (2012) 60–69

Contents lists available at SciVerse ScienceDirect

Journal of Molecular Graphics and Modelling

journal homepage: www.elsevier.com/locate/JMGM

Inhibitory activities and possible anticancer targets of Ru(II)-based complexes using computational docking method

Adebayo A. Adeniyi, Peter A. Ajibade*

Department of Chemistry, University of Fort Hare, Private Bag X1314, Alice 5700, South Africa

ARTICLE INFO

Article history:
Accepted 6 August 2012
Available online 14 August 2012

Keywords:
Docking
Ru(II)-based complexes
Selectivity
Cancer receptors
Carboxylic

ABSTRACT

In an effort to search for better alternatives to *cis*-platin and its derivatives that are non-selective cytotoxic anticancer agents, many metal based complexes especially that of Ru(II) that will have alternate targets other than universal target such as DNA have been suggested. This paper focus more on finding an alternative protein targets other DNA for some Ru(II)-based complexes using computational docking as a means of addressing commonly reported research challenges with regards to the lack of proper understanding of the anticancer targets of Ru-based complexes. The observed interactions through our docking studies showed that, besides predicted targets such as CatB, HP-NCP and kinase which is in good agreement with experiment since they have been experimentally suggested as possible target of Ru-based anticancer agents, other targets such as RNR and HDAC7 are proposed. Majority of the complexes on the average showed good interactions with rHA which will most likely enhance their pharmacokinetic properties. There is the possibility of some of them acting as anticancer and as antibacterial agent because they bind more favourably with DNA-Gyrase.

1. Introduction

In an effort to address the present problems in cancer therapy such as non selectivity of the cytotoxic cancer drugs, ineffectiveness towards many metastasised cancer cells, drug resistance and toxicity, many researchers are focusing on the design of better selective anticancer candidates of metal-based complexes due to the recorded success of *cis*-platin above all the available organic anticancer counterparts even though it is non-selective [1–4]. Dyson and his co-researchers are recognise with the design of Ru-based complexes of kinetically favourable PTA group with many derivatives of the type $[(\eta 6\text{-arene})RuCl(PTA)_2]$, $[(\eta 6\text{-cymene})RuCl(PTA)_2]$, $[CpRuCl(PTA)_2]$ and $[Cp^*RuCl(PTA)_2]$ synthesised and all these compounds have been reported to be similar in that they display only weak *in vitro* activity but better *in vivo* activity [5–9]. However, the complex RAPTA-C which is reported to show an excellent *in vivo* characteristic comparable to those of NAMI-A can only achieve that at higher doses [9]. There are still several research efforts in place to derive compounds of π-ligand, PTA and halide ligands that are more cytotoxic at lower doses and may reduce tumour mass *in vivo* [9]. Sadler and his co-researchers are also known for the "piano-stool" type of Ru-based complexes [10,11] which are often characterised with bidentate nitrogen donor atoms (*e.g.* ethylenediamine) coordinating with the metal. Both group of researchers are exploring the used of cyclic π-ligand with other ligands coordinated to Ru metal centre as potential anticancer agents. It has been observed that metal in a way has been enhancing and even inducing some pharmacological properties into ligands as some non-cytotoxic ligands such as PTA [3–9], ethylenediamine [10,11], and many others in complex metals lead to compounds with significant anticancer activity [12].

Our research efforts is directed towards proposing better selective anticancer agents by focusing more on cancer peculiar proteins other than DNA and also predict complexes that display higher activity at lower dose because most of the current anticancer complexes are only effective at high dose [9]. The search for the alternative targets for Ru-based complexes is a research challenge as the targets of many of these complexes cannot be ascertained [7,13–16]. The lack of proper understanding of the targets of Ru-based complexes is hindering their rational design [15] and it is the major factor that is hindering the NCI approval of Ru-based complexes such as indazolium *trans*-[tetrachloridobis(1H-indazole)ruthenate(III)] (KP1019), and imidazolium *trans*-[tetrachlorido(1H-imidazole)(S-dimethyl sulfoxide)ruthenate(III)] (NAMI-A) [6]. In this present work, we are interested in modelling of new forms of Ru-based complexes and to make a parallel comparison with some of the most effective rapta family especially the reported hydrated active forms with one chloride replaced by a single water molecule [11–13,3] and others with bidentate ligands, *i.e.* CraptaC and OraptaC. The essence of this is to possibly address the limitations of rapta complexes such as ineffectiveness until higher dose as reported in the literature

* Corresponding author. Tel.: +27 0 40 602 2055; fax: +27 0 86 518 12225.
E-mail address: pajibade@ufh.ac.za (P.A. Ajibade).

1093-3263/$ – see front matter © 2012 Elsevier Inc. All rights reserved.
http://dx.doi.org/10.1016/j.jmgm.2012.08.004

[9]. Therefore, to accomplish this we combine some features of the "piano-stool" from Sadler et al. [10,11] and "rapta" from Dyson et al. [5–9]. Also, we predicted a model with cyclopentadienyl (Cp) as a substitute for the arene group of the complexes to generate new Ru-based complexes due to the reported higher activities of compound of the type $[(Cp'OR)RuCl(PTA)_2]$ in two orders of magnitude than a close model structure with excellent activity in a *cis*-platin resistant cancer cell line [9]. Therefore, to gain deeper insight on the problems associated with variance of *in vivo* and *in vitro* behaviour of the potential Ru-based anticancer complexes [2,6], we analyse the interactions between ten receptors and the complexes theoretically. To the best of our knowledge, there has not been any serious computational study comparing the docking behaviour of these types of metal-based complexes with the chosen receptors and many of the predicted metal-based structures have not been considered.

In our effort to predict the possible target and the mechanism of the anticancer activities of Ru(II)-based complexes, ten different receptors of various relevance in cancer chemotherapy targets are considered. The receptors used are Recombinant Human albumin (rHA), Thymidylate synthase (TS), Ribonucleotide reductases (RNR), Histone Deacetylase (HDAC7), Cathepsin B (CatB), Topoisomerase 11 (Top 11), Thioredoxin reductase (TrxR), BRAF Kinase and Histone Protein in Nucleosome core particle (NCP) and DNA-Gyrase was included to study the possibility of anticancer complexes also acting as antibacterial agents. Their respective pdb files: 1BM0, 2G8D, 4R1R, 3C0Z, 1CSB, 1QZR, 1H6V, 3Q4C, 3MNN and 1AJ6 were obtained from protein database (pdb) [17]. Top II plays an important role in replication, transcription, recombination and segregation of chromosomal pairs during cell division. It has become a common target for a range of drugs, including anticancer, antimalarial and antiviral compounds [18,19]. TrxR system (TrxR reductase and NADPH) is a ubiquitous flavoenzyme of thiol oxidoreductase system that regulates cellular reduction/oxidation (redox) status [14,20]. TrxR is a likely pharmacological target for a range of metallodrugs because its active site selenolate group manifests a large propensity to react with "soft" metal ions after its reduction [14]. Also, the observation that there is over expression of TrxR in many aggressive tumours has recently lead to the suggestion of TrxR as a therapeutic target for cancer therapy [21]. BRAF kinase is one of the three members of RAF kinases that were originally identified as cellular homologues of v-raf oncogenes acquired by retroviruses. The remaining two of this member are: CRAF (RAF-1 or c-RAF-1) and ARAF. RAF kinases function by the activation of ERK1/2 as a subsequent effect of their specific phosphorylation of MEK1/2 within the kinase activation loop which leads to its activation [22]. The activated ERK1/2 translocates into the nucleus and activates transcription factors to promote cellular outcomes, including survival, growth, proliferation, and differentiation. BRAF KINASE represents an excellent target for anticancer drugs development because it differs significantly from other two members (CRAF and ARAF) as a major activator of MEK1/2 and requires fewer regulatory events for activation [22]. It has been found out that mutations notably V600E which is reported to account for 90% of cancer-associated BRAF mutations render the BRAF kinase constitutively active [22]. NCP has been pointed out as a basic repeating element of histone-packaged DNA comprising chromatin. Chromatin has become one of the potential superlative therapeutic targets for metallodrugs and other compounds because of its abundance and primary regulatory function of histone proteins and DNA sites [23]. Histone binding has been suggested to possibly contribute to the therapeutic activity of RAPTA compounds. It has also been reported that RAPTA-C treatment of the NCP results in three well defined histone binding sites [23]. DNA gyrase is included in this project to examine the possibility of anticancer agents also acting as antibacterial agents that may be relevant since bacterial infections are known to be opportunistic infections. DNA gyrase is a bacterial type II DNA topoisomerase (EC 5.99.1.3) and is found in all bacteria [24,25]. It controls the topological state of DNA [25] and uses the free energy of ATP hydrolysis to catalyse the negative super coiling of double-stranded circular DNA [24]. Since the relaxation of DNA is essential for DNA replication and transcription, therefore the inhibition of DNA blocks relaxation of super coiled DNA, which makes gyrase a suitable target for antibacterial agents [24,25]. The significant roles of other receptors used are discussed in the other part of our work.

2. Experimental method

There have been limitations in the application of docking to metal-based complexes which results in a very few reports in the literatures compare to organic compounds due to lack of appropriate force fields to take care of the metals [26] and their relativities and the difficulty of optimising the initial structures. In this research, the geometry of the Ru-based complexes used were first optimized with DFT method using Firefly package [27] with the procedures, the functional group and basis sets used reported in another part of our work. The optimized structure which is the first criteria for any possible successful docking of metal-based complexes were used for the two docking tools used which are the Autodock 4.2 suit [28] and the Glide 5.8 [29] package. The molecular graphics and other analyses were performed with the UCSF Chimera package [30].

In Autodock, the Lamarckian genetic algorithm is chosen because it has been pointed out to be most efficient, reliable and successful than others such as simulated annealing (SA) and a generic genetic algorithm (GA) methods in autodock [31,32]. For the Ru atom charge, we applied the native charge of +2 which is general and can be applied to any complex/receptor interaction study though it may not be as accurate as using an optimized charge which is more specific to the type of the system as it was reported for the docking of the metalloenzymes that contain Zn atom [26]. The active site was defined using AutoGrid version 4 and the grid size was set to $60 \times 60 \times 60$ points with a grid spacing of 0.375 Å centred on the selected residues of the binding site of each receptor. The grid box includes the entire binding site of the enzyme and provides enough space for the ligand translational and rotational walk. Step sizes of 2 Å for translation and 50° for rotation were chosen and the maximum number of energy evaluations was set to 1,750,000. Twenty runs were performed and for each of the 20 independent runs, a maximum number of 27,000 GA operations were generated on a single population of 100 individuals. Default values for the operator weights for crossover (0.80), mutation (0.02) and elitism (1.00) parameters were used.

The trial version of Glide [29,33] which is part of the as part of Maestro 9.3 suite of programs was also used for docking. The method use in Glide docking is referred to as funnel approach where a series of ligand conformations are initially created by Glide and then removing the unfavourable ones [34]. After this, refinement is performed by energy minimization followed by a restricted Monte Carlo search on the lowest energy conformations to refine the initial structure. The protein structures in mol2 format were prepared using the protein preparation wizard with default values and the incomplete residues of the receptors were corrected using Prime package [35]. Since, Glide ligand preparation package lack the force field to take care of metal-based complex, then protein preparation wizard was manipulated to prepare the metal-based complexes for docking as if the Ru(II) metal is a part of the protein. The Grids for the prepared protein were generated using 25 Å box with the centre of the grid being defined by using the ligand that is on the binding site of the protein and the force field used is

Table 1
The structures of the Ru(II)-based complexes as anticancer agents.

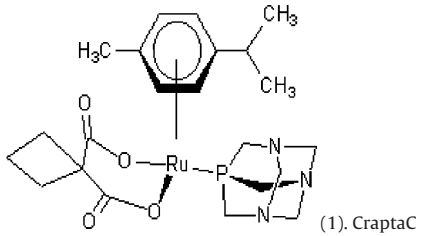
(1). CraptaC

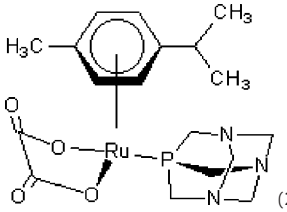
(2). OraptaC

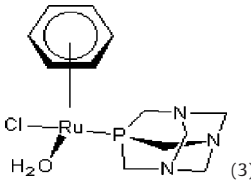
(3). RaptaB-H_2O

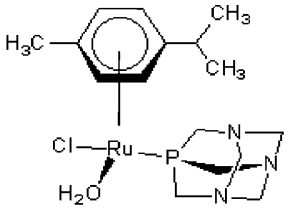
(4). RaptaC-H_2O

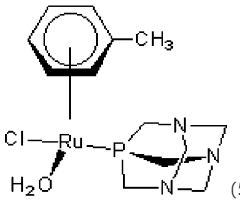
(5). RaptaT-H_2O

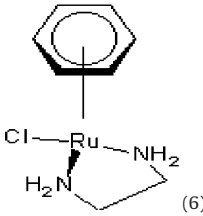
(6). Piano

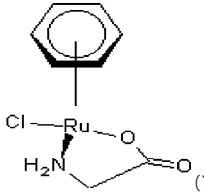
(7). Ragly

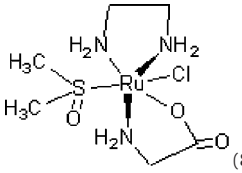
(8). Etdiaglydmso

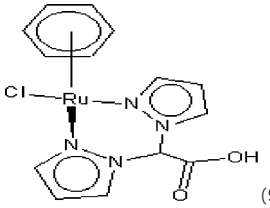
(9). Radipyrazoic

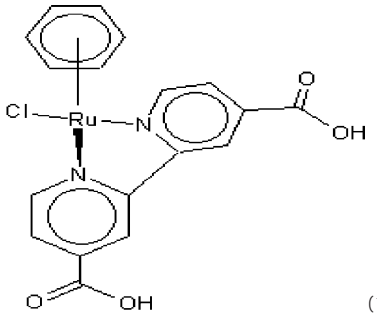
(10). Radipyrdioic

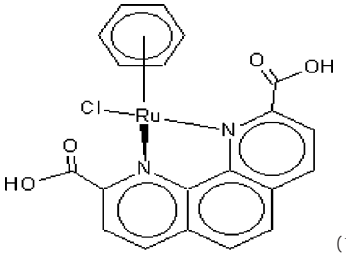
(11) Raphendioic

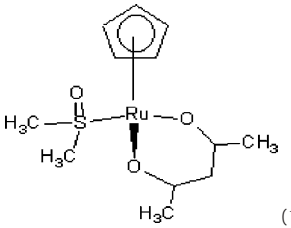
(12). Rcpbkdmso

Ra = Ruthenium-(η6-arene); etdia = ethylenediamine; phen = phenanthroline; pyr = pyridine; pyraz = pyrazole; PTA = 1,3,5-triaza-7-phosphaadamantane; Cp = cyclopentadienyl; bk = β-diketone; piano = model of piano-stool.

Table 2
The binding activities of the Ru(II)-based complexes as predicted suing Glide package.

		CatB	DNA-Gyrase	HDAC7	HP-NCP	KINASE	rHA	RNR	Top11	TrXR	TS
1	CraptaC	−2.14	−1.68	−1.41	−2.67	−3.45		−1.51		−1.70	−1.00
2	OraptaC	−2.19	−2.19	−2.38	−2.15	−4.44	−2.12	−0.55		−2.69	−3.71
3	RaptaB-H_2O	−4.04	−3.18	−2.16	−3.41	−3.10	−2.40	−3.52	−5.68		−4.10
4	RaptaC-H_2O	−3.56	−2.49	−3.35	−2.99	−2.61	−2.61	−3.64	−3.97	−2.37	−2.82
5	RaptaT-H_2O	−3.98	−2.48	−2.61	−2.87	−3.38	−2.23	−3.75	−4.75	−2.57	−3.76
6	Piano	−4.35	−3.41	−3.72	−3.29	−3.48	−3.75	−3.40	−4.96	−3.45	−3.94
7	Ragly	−2.92	−3.63	−2.73	−3.90	−4.83	−3.35	−2.06	−4.42	−2.88	−3.32
8	Etdiaglydmso	−2.57	−2.88	−2.12	−4.17	−4.02		−2.42	−3.79	−3.60	−3.52
9	Radipyrazoic	−4.93	−3.88	−3.40	−5.11	−3.12	−3.10	−7.10	−5.15	−4.43	−4.10
10	Radipyrdioic	−3.22	−4.60	−4.06	−4.00	−5.97	−3.57	−6.87	−3.87	−4.69	−4.00
11	Raphendioic	−4.37	−4.39	−2.62	−3.20	−4.30	−3.85	−4.71	−4.58	−3.33	−4.97

Table 3
The binding activities of the Ru(II)-based complexes as predicted suing Autodock package.

		CatB	DNA_Gyrase	HDAC7	HP-NCP	KINASE	rHA	RNR	top11	TrXR	TS
1	CraptaC	−9.29	−8.92	−8.33	−7.11	−6.57	−6.49	−5.49	−4.47	−5.22	−8.05
2	OraptaC	−9.11	−8.35	−7.93	−7.59	−6.44	−5.52	−5.16	−5.6	−5.96	−7.15
3	RaptaB-H_2O	−7.16	−6.21	−6.95	−6.78	−6.3	−4.72	−3.79	−4.41	−5.1	−5.46
4	RaptaC-H_2O	−8.15	−6.58	−6.63	−6.75	−6.21	−5.11	−3.89	−4.14	−4.78	−5.17
5	RaptaT-H_2O	−7.27	−6.26	−6.61	−7.01	−6.32	−5.04	−3.62	−4.42	−5.05	−5.52
6	Piano	−5.83	−5.56	−6.49	−7.31	−6.45	−5.35	−3.72	−4.53	−4.72	−4.26
7	Ragly	−5.63	−5.05	−5.77	−6.6	−5.08	−4.88	−3.64	−4.38	−5.04	−4.5
8	Etdiaglydmso	−9.34	−7.57	−8.63	−8.5	−7.92	−6.37	−4.02	−6.46	−6.3	−5.62
9	Radipyrazoic	−4.49	−3.77	−3.84	−3.94	−3.4	−4.3	−4.93	−4.73	−4.17	−4.5
10	Radipyrdioic	−3.68	−4.4	−2.5	−5.01	−5.33	−6.09	−5.65	−6	−6.24	−4.91
11	Raphendioic	−5.3	−5.58	−3.48	−5.49	−4.77	−6.52	−5.47	−5.48	−4.93	−5.04
12	Rcpbkdmso	−6.16	−5.6	−6.05	−4.85	−4.18	−4.63	−4.69	−4.35	−4.39	−4.73

OPLS_2005 which recognizes the metal atom. The default parameters in Glide for standard precision (SP) docking mode were used. In both Autodock and Glide dockings, flexibility of the complexes was allowed. The correlation table was derived using the statistical tool R (http://www.R-project.org).

3. Result and discussion

In this paper, we focus our interest on predicting the best targets for some of the Ru(II)-based complexes as anticancer agents which has being a great research challenge [2,7,13–16,6,36,37] and also try to compare the newly predicted hypothetical anticancer complexes with the known rapta complexes. The structure of the complexes that were docked into the binding sites of the proposed ten targets using Autodock and Glide docking is shown in Table 1. The analysis of the results obtained from Glide docking as shown in Table 2 gives the picture of the predicted inhibitory strength of the Ru(II)-based complexes used. The interest here is to compare some of the newly proposed structures with the best of existing rapta complexes using glide docking. The results showed that many of the complex-receptor binding activities preferentially predicted our newly proposed structures especially **9** and **10** to bind more favourably compare to the rapta type of complexes. These two complexes also showed the strongest binding with RNR, the best predicted inhibitors of RNR and also the best two inhibitors of TrXR in a reverse order.

Table 4
The correlation between the rankings of the complexes activity as predicted from Autodock and Glide packages.

	Autodock/Glide
CatB	−0.65
DNA-Gyrase	−0.86
HDAC7	−0.69
HP-NCP	−0.55
KINASE	−0.12
rHA	0.46
RNR	0.24
TopII	−0.55
TrXR	0.11
TS	−0.66

The best targeted receptors of the complexes with the highest activities are RNR (because of strong interaction of **9** and **10** only), Kinase (due to strong interaction of **10**, **7**, **2**, **11**, **8** and **1** in a decreasing order), Top11 (predicted as good target of most of the complexes except **1** and **2** where no activity is recorded) and CatB (mainly **9**, **11**, **6**, **3** and **5**), followed by HP-NCP, TS (but is a poor target of **1** and **4**), DNA-Gyrase and TrXR are average targets while HDAC7 and rHA are predicted to be relatively poor targets. The general features of the Glide docking shows that **9** and **10** followed by **6** are predicted as the best inhibitors of most of the receptors considered using Glide. The feature of the interaction of the complexes with CatB shows that besides our proposed **9**, **11**, and **6** the best of the rapta complexes are predicted to be **3**, **5** and **4** but **1** is predicted poor.

The suggested targets as most favourable of the complexes from the Autodock docking (Table 3) are CatB, HP-NCP, HDAC7 (except **9**, **10**, **11**), Kinase and DNA-Gyrase. Those suggested as average targets are TS (still one of the best targets for **1** and **2**), TrXR (the best target for **10**) and rHA (the best target for **11**) while RNR (part of the best target for **10** and **11**) and Top11 (but still a good target for **10**) are suggested as poor targets for most of the complexes. In line with the reported experimental results, Cat B is still the best predicted target of the rapta complexes in the order of **1**, **2** and **4** which is an indication that prediction of Autodock agree better with the experimental finding than Glide as **4** is experimentally proposed as having the best anticancer activity and interaction with CatB than many other rapta complexes [2,14]. This shows that **1** and **2** as derivative of **4** that can resist hydrolysis [7] interact more competitively with Cat B than the parent complexes. However, **8** among our complexes is predicted a better inhibitor of CatB than rapta complexes. Also, a critical look at the best predicted activities of the complexes across the best targets shows that complex **8** is predicted best inhibitor for Cat B, HP-NCP, HDAC7 while **1** and **2** are predicted better inhibitors than **8** for DNA-Gyrase which is a suggestion that rapta complexes

can equally act as antimalarial [24,25]. Therefore, in most cases the order of activities of the complexes follows as **8**, **1**, **2** and **4** as the best inhibitors.

However, the order of ranked best complexes may not be completely absolute since the reliability of the order for autodock is ~2.177 kcal/mol standard error [31,32] and the difference between the best ranked is not up to 2.1 kcal/mol (Table 2) as our chosen interval which is a little stringent than reported ~2.177 kcal/mol. Those that are still within the range of 2.1 kcal/mol as the predicted best inhibitor of HDAC7 are **8** followed by **1**, **2**, **3** and **4** respectively. The complexes **8**, **1**, **6**, **2**, **5** and **3** are respectively predicted as best for Kinase inhibition. Since rHA is known to help in the pharmacokinetic availability of a wide range of drugs, including metallodrugs and consequentially determine their bioavailability and toxicology [10], therefore the observed average interactions of the complexes with rHA is an indication that many of the Ru(II)-based complexes that are considered will averagely be kinetically favourable which is in good agreement with experimental findings [2,3,38]. However, **11** is taking the lead for rHA follow by **1**, **8** while for the inhibition of RNR, **10** takes the lead follow by **1** and **11**. For the receptor TrXR, **10** are taking the lead followed by **8**, **2**, **1**, **3**, **5** and **4** which shows little disparity from experimental ranking of the rapta complexes as inhibitors of TrXR [14]. However, the generally observed poor interaction of the rapta complexes with

Table 5
The interaction of the binding site residues with first two rank best inhibitor complexes from the three docking methods defining the complex–receptor existing hydrogen bond (HB) and metal–receptor (MR) possible interactions with residues within the range of 4.5 Å.

Receptor	Autodock	Glide
CatB	etdiaglydmso[a]{[HB: 2.31 Å (H^1@NH_2EtNH_2)-(O@CO CYC 26D)], [HB: 1.72 Å (H^2@NH_2EtNH_2)-(O@COOH GLU 122E)], [HB: 1.93 Å (H@NH_2CH_2COO)-(O@COOH GLU 122E)], [HB: 2.73 Å (N@NH_2CH_2COO)-(H@COOH GLU 122E)], [HB: 2.87 Å (O@NH_2CH_2COO)-(S@CH_2S CYS 29D)], [HB: 2.13 Å (O@NH_2CH_2COO)-(H@NH CYS 29D)], [MR: 3.38 Å (O@COOH GLU 122 E)], [MR: 4.36 Å (CH GLY 27 D)]}; CraptaC[b]{[HB: 1.92 Å (O@COO)-(H@im HIS 111E)], MR: 4.07Å (ar TRP 221E)};	radipyrazoic[a]{[HB: 1.82 Å (H@COOH)-(O@COO GLU 122E)], [MR: 3.66Å (H@ar TRP 221E)]}; raphendioic[b]{[HB: 1.63 Å (H@COOH)-(O@COO GLU 122E)], [MR: 4.27 Å (H@ar TRP 221E)]};
DNA-Gyrase	CraptaC[a] {[HB: 1.74Å (O@COO)-(H@NH VAL 120A)]; [MR: 4.35Å (NH2 ASN 46A)}; OraptaC[b] {[HB: 1.78Å (O@COO)-(H@NH VAL 120A)], [MR: 4.41Å (CO GLY 117A)], [MR: 4.48Å (CH2 GLY 119A)]};	radipyrdioic[a] {[HB: 2.12 Å (H@$COOH^1$)-(O@CO ASP 49A)]; [HB: 1.92 Å (O@$COOH^2$)-(H@NH GLY 77A)];[HB: 2.08 Å (H@$COOH^2$)-(O@CO ASP 73A)]; raphendioic[b] {[HB: 1.67 Å (H@$COOH^1$)-(O@COO ASP 49A)], [HB: 2.48 Å (H@$COOH^2$)-(O@COO ASP 73A)], [MR: 4.14Å (CH_2 ASN 46A)], [MR: 4.09 Å (CH2 ILE78A)]}
HDAC7	etdiaglydmso[a]{[HB: 1.67 Å (H@NH_2EtNH_2)-(O@COO ASP 626 A)], [MR: 4.06 Å (COO ASP 626 A)]}; CraptaC[b]{MR: 3.53Å (COO ASP 626 A)};	radipyrdioic[a] {[HB: 1.58 Å (H@COOH)-(O@COO ASP 626A)], [MR: 3.59 Å (H@CH_2 PHE 738 A)], [MR: 4.45 Å (H@NH PHE 738 A)], [MR: 4.36 Å (O@CO PRO 809 A)], [MR: 4.47 Å (H@CH_2 PRO 809 A)]}; piano[b] {[HB: 2.10 Å (H@NH_2)-(O@CO PRO 809 A)], [MR: 4.11 Å (H@CH_3 LEU 810 A)], [MR: 4.29 Å (O@CO PRO 809 A)], [MR: 4.35 Å ($H^{1,2}$@CH_2 PHE 738 A)]}
HP-NCP	etdiaglydmso[a]{[HB: 1.98 Å (O@DMSO)-(H@NH ASP 478 A)], [MR: 3.96 Å (O@COO GLU 532 A)], [MR: 4.42Å (O@COO ASP 478 A)]}; OraptaC[b] {[IT: 2.90 (N@PTA)-(O@COO GLU 64G)],[MR: 3.73Å (COO GLU 61G)]},	radipyrazoic[a] {[HB: 2.12 Å (O@COOH)-(H@COOH GLU 61 G)], [MR: 4.50 Å (H@COOH ASP 90 G)]}; etdiaglydmso[b] {[HB: 2.09 Å (O@COOH)-(HN@im HIS 106H)]}

Table 5 (*Continued*)

KINASE	etdiaglydmso[a] {[HB: 2.15 Å ($H@NH_2EtNH_2^1$)-(O@COO GLU 68 H)], [HB: 1.76 Å ($H@NH_2EtNH_2^2$)-(O@COO ASP 65 H)], [MR: 4.06 Å (CH_2COO ASP 65 H)]}; CraptaC[b] {[HB: 1.36 (O@COO)- (H@im HIS 584A)]};	radipyrdioic[a] {[HB: 2.55 Å ($H@COOH^1$)-(O@CO CYS 531A)], [HB: 2.10 Å ($O@COOH^1$)-(H@NH CYS 531A)], [HB: 2.67 Å (O@COOH2)-(H@OH THR 528A)], [MR: 3.88 Å ($H@CH_3$ VAL 470 A)], [MR: 4.28 Å (H@ar PHE 582 A)]}; ragly[b] {[HB: 1.99 Å (O@COO)-(H@NH ASP 593 A)], [MR: 4.05 Å ($H@CH_3$ LEU 513 A)], [MR: 3.60 Å (H@NH ASP 593 A)], [MR: 3.40 Å ($H@CH_2$ LYS 482 A)], [MR: 4.06 Å ($H@NH_3$ LYS 482 A)]}
rHA	raphendioic[a] {[HB: 2.15 Å (H@COOH1)-(H@COO GLU 425 A)], [HB: 1.72 Å ($H@COOH^2$)-(O@CO PRO 113 A)], [HB: 1.92 Å (O@COOH2)-(H@NH ARG 145 A)], [MR: 4.45 Å (CH_2 ARG 145 A)]}; CraptaC[b] {[MR: 4.05Å (NH2 ASN 109A)], [MR: 4.21Å (COOH GLU 425A)]};	raphendioic[a] {[HB: 2.20 Å ($O@COOH^1$)-($H@NH_2$ ARG 145 A)], [HB: 2.23 Å ($O@COOH^1$)-(H@OH GLU 141 A)], [HB: 1.84 Å (O@COOH2)-($H@NH_3$ LYS 137 A)], [HB: 1.67 Å (H@COOH2)-(O@COOH GLU 37 A)], [MR: 4.45 Å ($H@NH_3$ LYS 137 A)]}; piano[b] {[HB: 1.99 Å ($H@NH_2$)-(O@COOH ASP 107 A)], [MR: 4.32 Å (O@COOH ASP 107 A)], [MR: 4.45 Å ($H@NH_2$ ASN 111 A)]}
RNR	radipyrdioic[a] {[HB: 2.32 Å ($H@COOH^1$)-(O@CO ARG 251A)], [HB: 2.60 Å ($O^1@COOH^2$)-(H@NH THR 209 A)], [HB: 1.99 Å (O1@COOH2)-(H@OH SER 625A)], [HB: 2.13 Å (O2@COOH2)-(H@NH SER 625A)], [HB: 2.26 Å (O2@COOH2)-(H@NH THR 624 A)], [HB: 2.43 Å (O2@COOH2)-(H@NH GLU 623 A)]}; CraptaC[b] {[HB: 1.99Å (O@COO)- (H@NH THR 209A)], [HB: 2.55Å (N@PTA)-(H@COOH GLU 441A], }	radipyrazoic[a] {[HB: 2.09 Å ($O^1@COOH^1$)-(H@NH GLU 633 A)], [HB: 1.89 Å ($O^1@COOH$)-(H@NH THR 624 A)], [HB: 1.95 Å (O2@COOH)-(H@NH SER 625 A)], [MR: 3.59 Å (CH_3 LEU 464 A)], [MR: 4.46 Å ($H@CH_2$ SER 224 A)]}; radipyrdioic[b] {[HB: 2.51 Å ($O^1@COOH^1$)-($H@NH_3$ LYS 154A)], [HB: 2.31 Å ($O^2@COOH^1$)-($H@NH_3$ LYS 154A)], [HB: 2.50 Å ($O^2@COOH^1$)-(H@OH THR 209 A)], [HB: 1.70 Å ($H@COOH^2$)-(H@OH THR 624 A)], [HB: 1.44 Å ($H@COOH^2$)-(H@OH SER 224 A)], [MR: 3.90 Å (H@CH2OH SER 224 A)]}
TopII	etdiaglydmso[a]{[HB: 2.17 Å ($O@NH_2CH_2COO$)-(H@NH LEU 124 A)], [MR: 3.85 Å (im HIS 123 A)]}; radipyrdioic[b] {[HB: 1.79 Å ($H@COOH^1$)-(O@CO PHE 362 A)], [HB: 2.00 Å ($H@COOH^2$)-(O@CO THR 27 A)]}	raptaB-H_2O[a]{[HB: 1.83Å ($H@H_2O$)- (O@OH SER 128A)], [HB: 2.04Å ($H@H_2O$)- (O@CO ASN 129A)], [IT: 2.97Å (N@PTA)- (O@CO ASN 70A)], [MR: 3.66Å (NH SER 128A)]}, radipyrazoic[b] {[HB: 2.28 Å (O@COOH)-($H@NH_3$ LYS 147 A)], [HB: 2.23 Å (H@COOH)-(O@CO ASN 70 A)], [MR: 4.31 Å ($H@CH_3$ ILE 120A)], [MR: 4.01 Å (H@OH SER 128 A)]};

Table 5 (*Continued*)

TrXR	etdiaglydmso[a] {[HB: 1.83 Å (H@NH_2EtNH_2)-(O@CO THR 161 A)], [MR: 3.66 Å (CO THR 161 A)], [MR: 3.97 Å (O@CO PHE 43 A)], [MR: 4.21 Å (H@NH PHE 43 A)], [MR: 4.15 Å (H@NH GLY 20 A)]}; radipyrdioic[b] {[HB: 2.30Å (H@COOH[1])-(O@CO LEU 41 A)], [HB: 1.91 Å (H@COOH[2])-(O@CO ALA 160 A)], [HB: 2.11 Å (O1@COOH2)-(H@NH GLY 24 A)], HB: 2.43 Å (O2@COOH2)-(H@NH GLY 23 A)], [MR: 3.82 Å (H@NH_2 ARG 164 A)], [MR: 4.33 Å (O@CO THR 161 A)], [MR: 4.00 Å (H@NH TRP 53 A)], [MR: 4.10 Å (NH THR 58 A)], [MR: 3.41 Å (OH THR 58 A)]}	radipyrdioic[a] {[HB: 1.92 Å (O@COOH)-(H@COOH GLU 163 A)], [HB: 2.22 Å (H@COOH)-(O@CO ARG 293 A)], [MR: 3.81 Å (H@NH_2 ARG 166 A)]}; radipyrazoic[b] {[HB: 2.60 Å (O@COOH)-(H@COOH GLU 163 A)], [HB: 2.29 Å (O@COOH)-(H@NH_2 ARG 166 A)]}
TS	CraptaC[a] {[no HB and MR]}, OraptaC[b] {[HB: 1.86Å (O@COO)-(H@SH CYS 198A], [HB: 2.22Å (CO)-(H@NH ASP 221A], [MR: 4.14Å (CH_2 GLY 225A)]}	raphendioic[a] {[HB: 2.91 Å (O@COOH)-(H@NH_2 ASN 229 A)], [MR: 3.94 Å (H@NH_2 ASN 229 A)]} raptaB-H_2O[b]{[HB: 1.69Å (H@H_2O)- (H@OH ASP 257A)], [MR: 3.73Å (OH SER 219A)]}

The superscript "a" and "b" stands for the first and second rank complex of each macromolecule.

TrXR compare to CatB agrees well with the experimental finding [14] and the newly proposed structures **10** and **8** are predicted the best inhibitors of TrXR. For the receptor TS, **1** and **2** are predicted as its best inhibitor and none of our newly proposed structure appear within the range of 2 kcal/mol of the Autodock prediction. Generally, complex **9** is predicted as poor inhibitor of most of the complexes while on the contrary complexes **8**, **1**, **2** accordingly are predicted as the best inhibitors of most of the complexes.

There is a good agreement between the predicted behaviour of the receptors towards the complexes as predicted by the Autodock and Glide packages. Both predicted CatB and Kinases as good targets of most of the complexes and TS as average target. While DNA-Gyrase, TrXR, and HP-NCP are either predicted as an average or one of the best by each of the two methods. These are in good agreement with the experimental findings as CatB [14], HP-NCP [23] and Kinase [22] have been suggested as possible targets of Ru(II)-based complexes. Also, the prediction of TrXR as less preferred target compared to CatB by both Glide and Autodock docking agree well with experimental report especially for rapta complexes [14]. However, there is disparity in the prediction of receptors RNR and Top11 which Autodock predicted as poor targets of the complexes but predicted by Glide as part of the best targets though they both still predict **10** as the best inhibitor of RNR. Also HDAC7 that Glide predicted as a poor target is taking to be one of the best in Autodock. There is a very wide disparity between their rankings of the inhibitory activities of the complexes as the leading complexes through the Glide prediction are **9**, **10**, **3**, **6**, **11**, **5** and **8** while the leading complexes in Autodock are **8**, **1**, **2**, **4**, **5** and **3**. The correlation of ranking order of the complexes from Autodock and Glide in Table 4 further gave a clear picture of the disparity in their ranking as most of the correlation determined for each receptor are highly negative which is an indication that the ranking of the complex activities by the two method are nearly reverse of each other. However, the comparison between the activities of the complexes predicted by the two methods of docking are not of interest, but the interest is to understand and to predict the optimal orientation and conformation of the complexes embedded in a proteins which is the primary objective of all the research efforts in the area of protein–ligand interactions, development of many different techniques and the associated software tools [32]. Also, being careful of the inherent inaccuracies in the calculated estimates of the binding energy by each of the different docking method, the binding energy cannot be directly compared and used for hit-ranking since the values are calculated using different docking programs with different force-fields [39].

In order to gain better insight into the binding site interaction and orientation of the complexes, a more critical look is presented in Table 5 for the best two inhibitors of each receptor in terms of hydrogen bond (HB) and metal–receptor (MR) possible interactions with residues within the range of 4.5 Å. The result from Glide docking shows that the orientation of the best two inhibitors of Cat B are alike with the carboxylic unit forming hydrogen bond with carboxylic unit of the GLU 122E. A likewise orientation also occur in the binding of the best two predicted inhibitors of DNA-Gyrase as the two inhibitors have common hydrogen bond interaction with ASP 73. The complex predicted as first of this two has no residue within the 4.5 Å of the metal radius that would possibly suggest any MR relationship. In HP-NCP the two complexes are characterised with single HB and MR with one oxygen unit of the COO group of **8** interacting with the NH unit of the imidazole group of HIS 106 H. In interaction of complexes with Kinase, **7** that is ranked second is found to penetrate further into receptor and characterised with many possible MR interactions (some are presented in Table 5) than **10** that was ranked first. The binding sites located on rHA by the two ranked best (**11** and **6**) are very widely separated from each other. The relative importance of MR interactions and other possible interactions with HB interaction is shown in the interaction of **6** with rHA where there is only single HB with higher MR compare with **11** (Table 5) where there is higher HB and yet their interacting energy is very close as shown in Table 2. The two best ranked complexes (*i.e.* **9** and **10** in that order) for RNR are found to penetrate more inside the receptor than the rest of the complexes. The

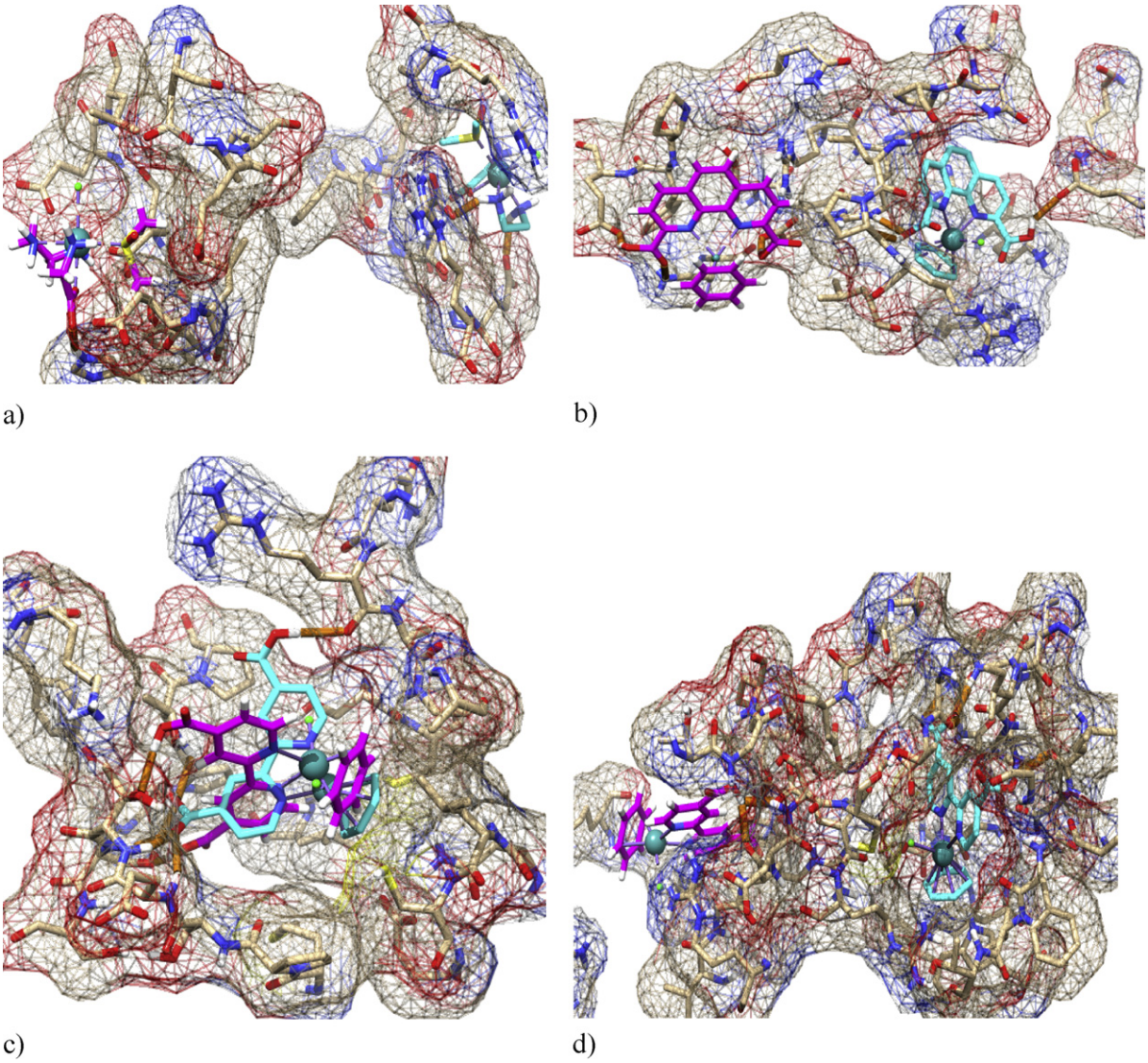

Fig. 1. The binding site interactions of one of the best two inhibitors of HP-NCP, rHA, RNR and TrXR as predicted by the Glide (left side with C atoms in magenta) and Autodock (right side with C atoms in cyan) showing hydrogen bond (orange cylinder form). (a) The interaction of etdiaglydmso with HP-NCP (in surface mesh) using Autodock and Glide; (b) the interaction of raphendioic with rHA (in surface mesh) using Autodock and Glide; (c) the interaction of radipyrdioic with RNR (in surface mesh) using Autodock and Glide; and (d) the interaction of radipyrdioic with TrXR (in surface mesh) using Autodock and Glide.

interaction of these two complexes is characterised with the lowest energy compare to the rest of complexes inhibiting any of the receptors. The feature of the interaction of these two complexes with RNR shows that the major factor that determined high stability and lowest energy is combination of HB and MR interaction as **10** that is ranked second have five HB while **9** that is ranked first have only three HB but two MR interactions. This is an indication that, besides the other possible interactions such as *van der waal*, electrostatic and steric, a well positioned HB by introducing carboxylic group into complexes coupled with possibility of MR can play a significant role in the anticancer activities of complexes. The interaction of the **3** and **9** as the best two inhibitors of Top II shows that the complexes penetrate well into the cavity of the receptor and characterised with higher number of HB which makes the interaction the second overall best after the interaction of the best two of RNR.

Also, the observations from Autodock further give insight into the biding site interaction of the complexes. A critical look at the interacting feature of the complexes with HDAC7 in relation to CatB (Table 5) indicates that though the inhibitory activities of their best two inhibitors are very closed (Table 3) yet the HDAC7 inhibitors are characterised with very few HB and MR which is an indication that there are other factors that are playing significant role on the inhibitory activities of complexes. In HP-NCP there is possibility of a very strong MR interaction as the side group of ASP 65A (*i.e.* CH_2COO) is having a closed and free space interaction with the Ru(II) metal. The sites of binding of the best two inhibitors of Top II are widely separated from each other suggesting two possible binding sites. The high inhibitory activities of the best two inhibitors of DNA-Gyrase and HDAC7 despite very few numbers of HB and MR interaction coupled with the best for TS where there is no recorded HB and MR shows the significant effects of other types of possible interactions.

There is further similarity between Autodock and Glide in the best two inhibitors that are predicted for some of the receptors as **8** is commonly predicted for receptor HP-NCP, **11** for rHA, **10** for RNR and **10** for TrXR (Table 5 and Fig. 1). A more critical look at these four receptors with the same complexes predicted among the best two,

the binding site located by Autodock for the complexes are different form Glide predicted binding site in HP-NCP, rHA and TrXR but the same in RNR as shown in Fig. 1. The orientation of **10** on the binding site of RNR as predicted by Autodock and Glide is very similar with the carboxylic units contributing to the stability by forming HB as shown in Fig. 1c. As shown in Fig. 1, all the four interactions of complexes with receptors are characterised with multiple HB (represented by orange cylinder shape). The different binding sites suggested by Autodock and Glide for the interaction of some complexes with some receptor give the possibility of having more than one binding site as it is even observed within the same package when Glide suggested different site for the best two inhibitors of rHA and Autodock suggest widely separated binding sites for the best two inhibitors of Top II. This is not far from the experimental report of multiple binding sites for Ru(II)-based complexes with HP-NCP [23] and Kinase [22].

4. Conclusion

In conclusion, the general feature shows that the inhibitory activities does not directly depend on the number of the HB nor number of the MR but on their strength and other possible interactions that could not be directly accounted for. Also, there is preference for better HB in the interactions of the complexes with receptor residues than assuming an orientation that would allow close MR interaction. Autodock docking shows that the newly proposed Ru(II) complexes especially **8**, **10** and **11** are better inhibitors of most of the receptors than rapta's complexes except receptor TS where none of the newly proposed structures could appear within autodock range of 2.1 kcal/mol error of best predicted inhibitors for TS. In addition, Glide docking also gives preference to some of the newly proposed complexes **8**, **9**, **10** and **11** as inhibitors of most of the receptors than many of the rapta's complexes. One of the observed reasons for the preferential binding of the newly proposed structures is observed to be the result of enhanced HB especially through the presence of carboxylic group in some of the new complexes. Autodock docking also suggested other receptors that can possibly be the targets of most of the Ru(II)-based complexes to be HDAC7 and TS which have not been considered specifically for rapta complexes to the best of our knowledge. Also, high activities of raptas with DNA-Gyrase according to autodock prediction is an indication that these complexes can equally act as antimalarial. Besides experimentally established possible anticancer target of Ru(II)-based complexes as CatB, other suggested targets are HDAC7, Kinase, TS and HP-NCP. Also, RNR as a rare anticancer target of many complexes is predicted as alternative anticancer target for the newly proposed complexes **9** and **10**.

References

[1] M. Groessl, Y.O. Tsybin, C.G. Hartinger, B.K. Keppler, P.J. Dyson, Ruthenium versus platinum: interactions of anticancer metallodrugs with duplex oligonucleotides characterised by electrospray ionisation mass spectrometry, Journal of Biological Inorganic Chemistry 15 (2009) 677–688.

[2] S. Chatterjee, S. Kundu, A. Bhattacharyya, C.G. Hartinger, P.J. Dyson, The ruthenium(II)–arene compound RAPTA-C induces apoptosis in EAC cells through mitochondrial and p53–JNK pathways, Journal of Biological Inorganic Chemistry 13 (2008) 1149–1155.

[3] A.E. Egger, C.G. Hartinger, A.K. Renfrew, P.J. Dyson, Metabolization of [Ru(η6-$C_6H_5CF_3$)(pta)Cl_2]: a cytotoxic RAPTA-type complex with a strongly electron withdrawing arene ligand, Journal of Biological Inorganic Chemistry 15 (2010) 919–927.

[4] C.S. Allardyce, P.J. Dyson, D.J. Ellis, S.L. Heath, [Ru(η6-p-cymene)Cl_2(pta)] (pta = 1,3,5-triaza-7-phosphatricyclo-[3.3.1.1]decane): a water soluble compound that exhibits pH dependent DNA binding providing selectivity for diseased cells, Chemical Communications (2001) 1396–1397.

[5] P.J. Dyson, G. Sava, Metal-based antitumour drugs in the post genomic era, Dalton Transactions 23 (2006) 1929–1933.

[6] G. Sava, A. Bergamoa, P.J. Dyson, Metal-based antitumour drugs in the post-genomic era: what comes next? Dalton Transactions 40 (2011) 9069–9075.

[7] C.S. Allardyce, A. Dorcier, C. Scolaro, P.J. Dyson, Development of organometallic (organo-transition metal) pharmaceuticals, Advances in Organometallic Chemistry 19 (2005) 1–10.

[8] C.S. Allardyce, P.J. Dyson, D.J. Ellis, S.L. Heath, [Ru(6-p-cymene)Cl_2(pta)] (pta = 1,3,5-triaza-7-phosphatricyclo-[3.3.1.1]decane): a water soluble compound that exhibits pH dependent DNA binding providing selectivity for diseased cells, Chemical Communications (2001) 1396–1397.

[9] B. Dutta, C. Scolaro, R. Scopelliti, P.J. Dyson, K. Severin, Importance of the π-ligand: remarkable effect of the cyclopentadienyl ring on the cytotoxicity of ruthenium pta compounds, Organometallics 27 (2008) 1355–1357.

[10] W. Hu, Q. Luo, X. Ma, K. Wu, J. Liu, Y. Chen, S. Xiong, J. Wang, P.J. Sadler, F. Wang, Arene control over thiolate to sulfinate oxidation in albumin by organometallic ruthenium anticancer complexes, Chemistry: A European Journal 15 (2009) 6586–6594.

[11] F. Wang, A. Habtemariam, E.P.L. van der Geer, R. Fernandez, M. Melchart, R.J. Deeth, R. Aird, S. Guichard, F.P.A. Fabbiani, P. Lozano-Casal, I.D.H. Oswald, D.I. Jodrell, S. Parsons, P.J. Sadler, Controlling ligand substitution reactions of organometallic complexes: tuning cancer cell cytotoxicity, Proceedings of the National Academy of Sciences of the United States of America 102 (2005) 18269–18274.

[12] M. Hanif, H. Henke, S.M. Meier, S. Martic, M. Labib, W. Kandioller, M.A. Jakupec, V.B. Arion, H. Kraatz, B.K. Keppler, C.G. Hartinger, Is the reactivity of M(II)-arene complexes of 3-hydroxy-2(1H)-pyridones to biomolecules the anticancer activity determining parameter? Inorganic Chemistry 49 (2010) 7953–7963.

[13] G. Gasser, I. Ott, N. Metzler-Nolte, Organometallic anticancer compounds, Journal of Medicinal Chemistry 54 (2011) 3–25.

[14] A. Casini, C. Gabbiani, F. Sorrentino, M.P. Rigobello, A. Bindoli, T.J. Geldbach, A. Marrone, N. Re, C.G. Hartinger, P.J. Dyson, L. Messori, Emerging protein targets for anticancer metallodrugs: inhibition of thioredoxin reductase and cathepsin B by antitumor ruthenium(II)-arene compounds, Journal of Medicinal Chemistry 51 (2008) 6773–6781.

[15] S. Page, Ruthenium compounds as anticancer agents, Education in Chemistry (2012) 26–29, www.rsc.org/eic

[16] C.S. Allardyce, P.J. Dyson, Ruthenium in medicine: current clinical uses and future prospects, Platinum Metal 45 (2) (2001) 62–69.

[17] Research Collaboratory for Structural Bioinformatics (RCSB) (2012), Online pdb database: www.rcsb.org

[18] Y.N.V. Gopal, D. Jayaraju, A.K. Kondapi, Inhibition of topoisomerase II catalytic activity by two ruthenium compounds: a ligand-dependent mode of action, Biochemistry 38 (1999) 4382–4388.

[19] G. Arpino, D.R. Ciocca, H. Weiss, D.C. Allred, P. Daguerre, L. Vargas-Roig, M. Leuzzi, F. Gago, R. Elledge, S.K. Mohsin, Predictive value of apoptosis, proliferation, HER-2, and topoisomerase IIa for anthracycline chemotherapy in locally advanced breast cancer, Breast Cancer Research and Treatment 92 (2005) 69–75.

[20] C.J. World, H. Yamawaki, B.C. Berk, Thioredoxin in the cardiovascular system, Journal of Molecular Medicine 84 (2006) 997–1003.

[21] C. Cadenas, D. Franckenstein, M. Schmidt, M. Gehrmann, M. Hermes, B. Geppert, W. Schormann, L.J. Maccoux, M. Schug, A. Schumann, C. Wilhelm, E. Freis, K. Ickstadt, J. Rahnenführer, J.I. Baumbach, A. Sickmann, J.G. Hengstler, Role of thioredoxin reductase 1 and thioredoxin interacting protein in prognosis of breast cancer, Breast Cancer Research 12 (2010) R44.

[22] P. Xie, C. Streu, J. Qin, H. Bregman, N. Pagano, E. Meggers, R. Marmorstein, The crystal structure of BRAF in complex with an organoruthenium inhibitor reveals a mechanism for inhibition of an active form of BRAF kinase, Biochemistry 48 (2009) 5187–5198.

[23] B. Wu, M.S. Ong, M. Groessl, Z. Adhireksan, C.G. Hartinger, P.J. Dyson, C.A. Davey, A ruthenium antimetastasis agent forms specific histone protein adducts in the nucleosome core, Chemistry: A European Journal 17 (2011) 3562–3566.

[24] G.A. Holdgate, A. Tunnicliffe, W.H.J. Ward, S.A. Weston, G. Rosenbrock, P.T. Barth, I.W.F. Taylor, R.A. Pauptit, D. Timms, The entropic penalty of ordered water accounts for weaker binding of the antibiotic novobiocin to a resistant mutant of DNA gyrase: a thermodynamic and crystallographic study, Biochemistry 36 (1997) 9663–9673.

[25] S. Ghaneya, G.S. Hassan, A. Nahla, N.A. Farag, H. Gehan, G.H. Hegazy, K. Reem, R.K. Arafa, Design and synthesis of novel benzopyran-2-one derivatives of expected antimicrobial activity through DNA gyrase-B inhibition, Archiv der Pharmazie: Chemistry in Life Sciences 341 (2008) 725–733.

[26] X. Hu, W.H. Shelver, Docking studies of matrix metalloproteinase inhibitors: zinc parameter optimization to improve the binding free energy prediction, Journal of Molecular Graphics and Modelling 22 (2003) 115–126.

[27] A.A. Granovsky, Firefly, Version 7.1.G, Copyright 1994, Firefly Project, Moscow, Russia, 2009, http://classic.chem.msu.su/gran/firefly/index.html

[28] G.M. Morris, R. Huey, W. Lindstrom, M.F. Sanner, R.K. Belew, D.S. Goodsell, A.J. Olson, Autodock4 andAutoDockTools4: automated docking with selective receptor flexibility, Journal of Computational Chemistry 30 (16) (2009) 2785–2791.

[29] R.A. Friesner, J.L. Banks, R.B. Murphy, T.A. Halgren, J.J. Klicic, D.T. Mainz, M.P. Repasky, E.H. Knoll, D.E. Shaw, M. Shelley, J.K. Perry, P. Francis, P.S. Shenkin, Glide: new approach for rapid, accurate docking and scoring. 1. Method and assessment of docking accuracy, Journal of Medicinal Chemistry 47 (2004) 1739–1749.

[30] E.F. Pettersen, T.D. Goddard, C.C. Huang, G.S. Couch, D.M. Greenblatt, E.C. Meng, T.E. Ferrin, UCSF Chimera—a visualization system for exploratory

research and analysis, Journal of Computational Chemistry 25 (13) (2004) 1605–1612.
[31] G.M. Morris, D.S. Goodsell, R.S. Halliday, R. Huey, W.E. Hart, R.K. Belew, A.J. Olson, Automated docking using a Lamarckian genetic algorithm and an empirical binding free energy function, Journal of Computational Chemistry 19 (14) (1998) 1639–1662.
[32] N.A. Caballero, F.J. Meléndez, A. Niño, C. Muñoz-Caro, Molecular docking study of the binding of aminopyridines within the K^+ channel, Journal of Molecular Modeling 13 (2007) 579–586.
[33] T.A. Halgren, R.B. Murphy, R.A. Friesner, H.S. Beard, L.L. Frye, W.T. Pollard, J.L. Banks, Glide: new approach for rapid, accurate docking and scoring. 2. Enrichment factors in database screening, Journal of Medicinal Chemistry 47 (2004) 1750–1759.
[34] C.R. Corbeil, N. Moitessier, Docking ligands into flexible and solvated macromolecules. 3. Impact of input ligand conformation, protein flexibility, and water molecules on the accuracy of docking programs, Journal of Chemical Information and Modeling 49 (2009) 997–1009.
[35] M.P. Jacobson, D.L. Pincus, C.S. Rapp, T.J.F. Day, B. Honig, D.E. Shaw, R.A. Friesner, A hierarchical approach to all-atom protein loop prediction, Proteins 55 (2004) 351–367.
[36] P. Heffeter, K. Bock, B. Atil, M.A.R. Hoda, W. Korner, C. Bartel, U. Jungwirth, B.K. Keppler, M. Micksche, W. Berger, G. Koellensperger, Intracellular protein binding patterns of the anticancer ruthenium drugs KP1019 and KP1339, Journal of Biological Inorganic Chemistry 15 (2010) 737–748.
[37] C.G. Hartinger, M.A. Jakupec, S. Zorbas-Seifried, M. Groessl, A. Egger, W. Berger, H. Zorbas, P.J. Dyson, B.K. Keppler, KP1019: a new redox-active anticancer agent—preclinical development and results of a clinical phase I study in tumor patients, Chemistry & Biodiversity 5 (2008) 2140–2155.
[38] W.H. Ang, E. Daldini, C. Scolaro, R. Scopelliti, L. Juillerat-Jeannerat, P.J. Dyson, Development of organometallic ruthenium–arene anticancer drugs that resist hydrolysis, Inorganic Chemistry 45 (2006) 9006–9013.
[39] D.-L. Ma, V.P.-Y. Ma, D.S.-H. Chan, K.-H. Leung, H.-J. Zhong, C.-H. Leung, In silico screening of quadruplex-binding ligands, Methods 57 (2012) 106–114.